ELSEVIER

Marine Geology 185 (2002) 319–340

MARINE GEOLOGY
INTERNATIONAL JOURNAL OF MARINE GEOLOGY, GEOCHEMISTRY AND GEOPHYSICS

www.elsevier.com/locate/margeo

# The Saguenay Fjord, Quebec, Canada: integrating marine geotechnical and geophysical data for spatial seismic slope stability and hazard assessment

Roger Urgeles [a,b,*], Jacques Locat [a], Homa J. Lee [c], Francis Martin [a]

[a] *Département de géologie et de génie géologique, Université Laval, Pavillon Pouliot, Ste. Foy, QC, Canada G1K 7P4*
[b] *GRC Geociències Marines, Departament d'Estratigrafia i Paleontologia, Universitat de Barcelona, Campus de Pedralbes, 08028 Barcelona (Catalonia), Spain*
[c] *United States Geological Survey, Mail Stop 999, 345 Middlefield Road, Menlo Park, CA 94025, USA*

Received 13 February 2001; accepted 15 January 2002

**Abstract**

In 1996 a major flood occurred in the Saguenay region, Quebec, Canada, delivering several km$^3$ of sediment to the Saguenay Fjord. Such sediments covered large areas of the, until then, largely contaminated fjord bottom, thus providing a natural capping layer. Recent swath bathymetry data have also shown that sediment landslides are widely present in the upper section of the Saguenay Fjord, and therefore, should a new event occur, it would probably expose the old contaminated sediments. Landslides in the Upper Saguenay Fjord are most probably due to earthquakes given its proximity to the Charlevoix seismic region and to that of the 1988 Saguenay earthquake. In consequence, this study tries to characterize the permanent ground deformations induced by different earthquake scenarios from which shallow sediment landslides could be triggered. The study follows a Newmark analysis in which, firstly, the seismic slope performance is assessed, secondly, the seismic hazard analyzed, and finally an evaluation of the seismic landslide hazard is made. The study is based on slope gradients obtained from EM1000 multibeam bathymetry data as well as water content and undrained shear strength measurements made in box and gravity cores. Ground motions integrating local site conditions were simulated using synthetic time histories. The study assumes the region of the 1988 Saguenay earthquake as the most likely source area for earthquakes capable of inducing large ground motions in the Upper Saguenay region. Accordingly, we have analyzed several shaking intensities to deduce that generalized sediment displacements will begin to occur when moment magnitudes exceed 6. Major displacements, failure, and subsequent landslides could occur only from earthquake moment magnitudes exceeding 6.75. 

*Keywords:* slope stability; seismic loading; Newmark analysis; contaminated sediments; Saguenay Fjord

## 1. Introduction

Fjords have been designated one of the major submarine landslide areas (Hampton et al., 1996) because of the rapid sediment deposition taking

* Corresponding author.
*E-mail address:* roger@beagle.geo.ub.es (R. Urgeles).

0025-3227/02/$ – see front matter 
PII: S0025-3227(02)00185-8

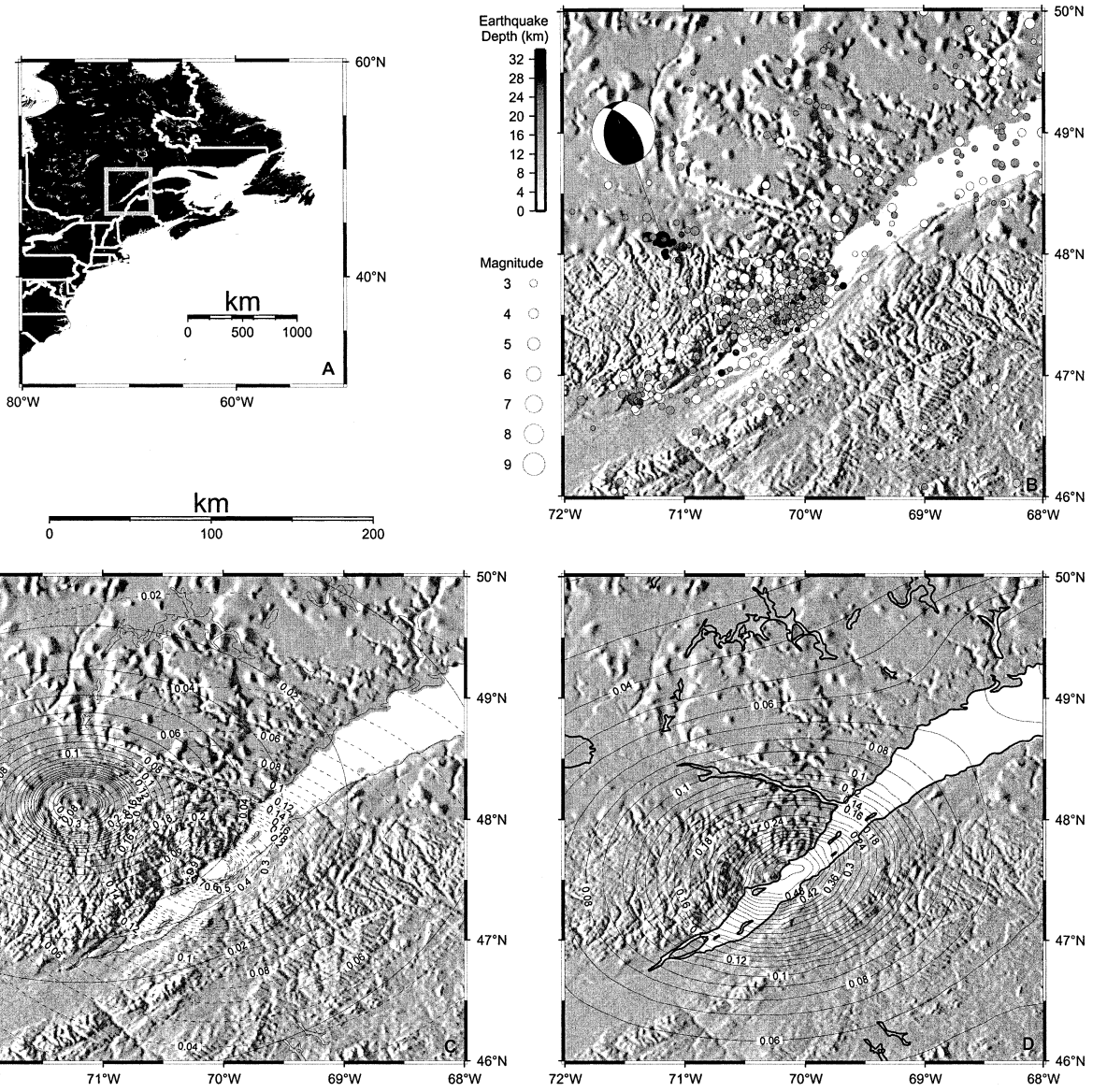


Fig. 1. (A) Location of the study area. (B) Earthquake epicenters from 1663 to present (Natural Resources Canada, 1999). Size of circle is proportional to earthquake magnitude ($M_n$) and gray scale is proportional to earthquake depth except for old earthquakes for which source depth is not known and which are represented in white. Moment tensor is plotted for the 1988 Saguenay earthquake (Department of Earth and Planetary Sciences, 2000). (C) Estimated earthquake acceleration for the Saguenay earthquake of 1988 (normal lines) as well as for the 1663 Charlevoix seismic event (dashed lines). Calculations of the peak ground acceleration (PGA) are presented as a fraction of $g$ and made according to attenuation equations as described in Atkinson and Boore (1995). Isolines appear as ovals because of the equidistant cylindrical projection. (D) PGA with 10% probability of exceedence in 50 years (Frankel et al., 1996). Background is topographic data from the GTOPO30 database (Earth Resources Information Systems Data Center, 1996).

place at their head deltas and their steep side walls. On the other hand, they provide protected ports and staging areas in rugged terrain which make them especially appealing for human activities. The combination of these two attributes makes them potential high landslide risk areas and emphasizes the need for geotechnical studies of such areas.

Earthquakes are also recognized as one of the major destabilizing factors in the marine environment (Hampton et al., 1996; Roberts and Cramp, 1996; Duperret et al., 1995; Piper et al., 1999). Earthquakes induce horizontal and vertical accelerations, which produce a direct load of the sediment. In addition, they induce a buildup of fluid pore pressure in the sediments, which leads to a strength reduction.

The Saguenay Fjord is thus an area where potential destabilization by earthquakes is significant, firstly because of the high sedimentation rates that take place at the fjord head, about 7 cm/yr (Schafer et al., 1980), and secondly because of the moderate seismic activity that this area and the neighboring region of Charlevoix experience (Fig. 1).

There was and there is still important industrial activity at the head of the Saguenay Fjord. These industries were a source of mercury and other metals (Loring and Bewers, 1978; Barbeau et al., 1981a,b), as well as aromatic hydrocarbons

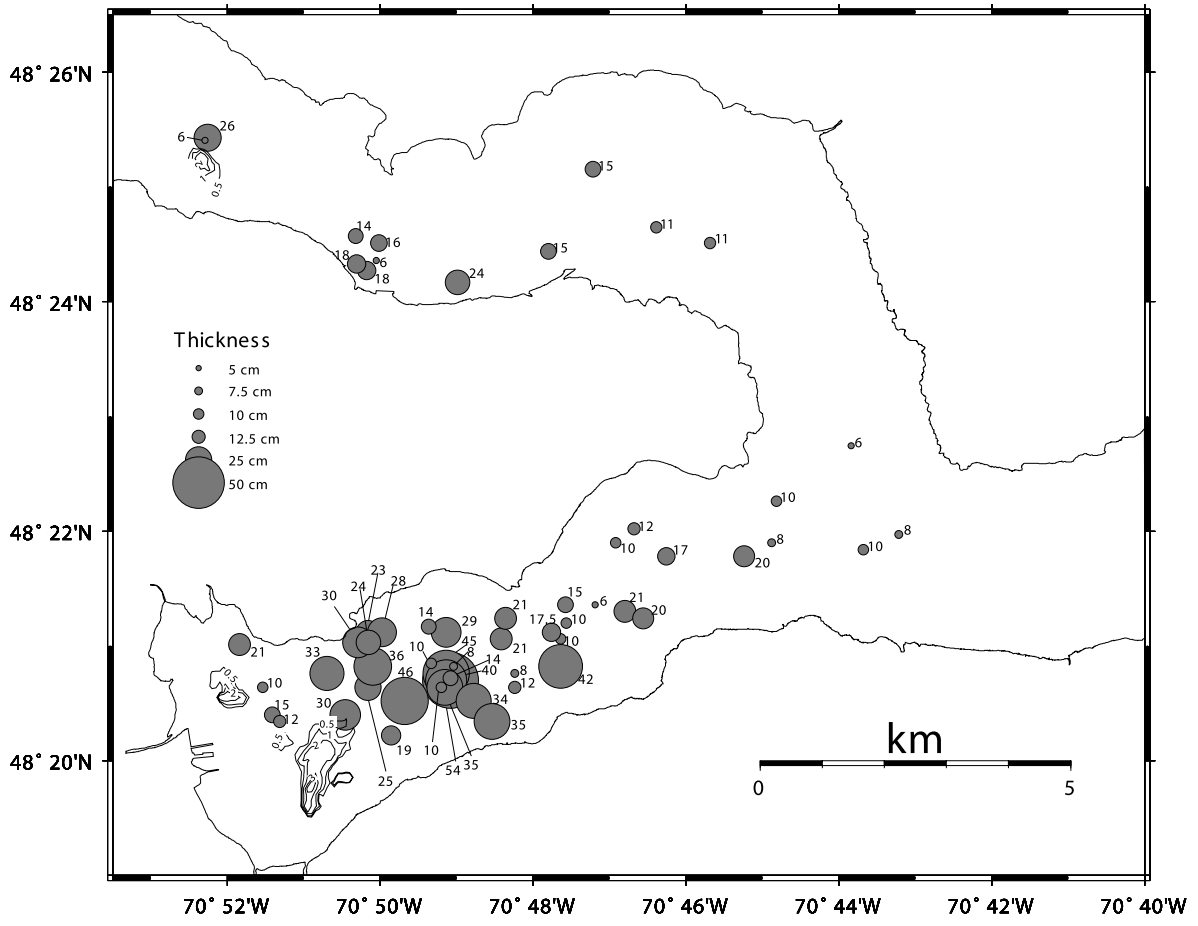


Fig. 2. Extent of the deposits of the 1996 flood. Isocontours are shown for areas where layer thickness is higher than 0.5 m, derived by coupling swath bathymetry data acquired in 1993 (previous to the flood) with data from 1999. For thicknesses lower than 0.5 m the thickness is shown as proportional circles indicating the thickness measured in the box cores.

(Martel et al., 1987), which were responsible for significant contamination of the fjord sediments.

In 1996 a major rainstorm and general flooding of the upper Saguenay region occurred, depositing a flood layer of 10–20 cm on average (Fig. 2), but reaching several meters near the river mouths where rivers directly discharged their material to the fjord (Fig. 2). The magnitude of the flood inspired a research project focused on evaluating the concealing of old contaminated fjord sediment and the stability of the new 'flood layer'. In contrast to the great damage the flood caused (Brooks and Lawrence, 1999), it was believed that the huge amount of 'clean' newly deposited flood sediments would bury the old contaminated ones, thus providing a natural capping layer. A major goal of these investigations was to evaluate the stability of the newly deposited layer since the recurrence of new landslide events could lead to the exposure of the old contaminated materials. In this study we tackle the issue of shallow landslide hazard which would most likely expose the 'old' contaminated sediments. In this paper we consider a seismic gravity loading approach following a Newmark (1965) analysis. On land, several examples of earthquake triggered landslides occurred during the 1988 seismic event (Tuttle et al., 1990; Lefebvre et al., 1992) and several older landslides and liquefaction structures are also attributed to seismic activity (LaSalle and Chagnon, 1968; Schafer and Smith, 1987; Chagnon and Locat, 1988; Locat and Bergeron, 1988; Locat et al., 1997, 2000). An additional factor, not considered in this study, that could induce slope failure in the Saguenay Fjord, especially at the river mouths, is the rapid deposition of large amounts of new sediment, as might occur during a new flooding event. Wave loading is not expected to produce landslides given the small area (the fjord has a maximum width of 3 km in this area) for wave generation and the great fjord depths (up to 200 m).

## 2. Geological framework

The Saguenay Fjord lies within the Canadian Shield, which is mostly composed in this area of metamorphic Precambrian rocks. The region was tectonically active between 175 and 190 Ma ago, which allowed the formation of the Saguenay graben (Du Berger et al., 1991). During the Pleistocene, the area was covered several times by ice sheets (LaSalle and Tremblay, 1978). The Saguenay graben, oriented more or less parallel to the glacial flow, became a preferred path for ice flow and resulted in deep excavation of the bedrock. The final retreat of the Wisconsinian ice sheet, which took place about 10 000 years ago (LaSalle and Tremblay, 1978), was followed by significant isostatic rebound, varying from 140 m on the north side of the graben to 120 m on the south side (Bouchard et al., 1983). The rebound was also accompanied by rapid infill of the graben with as much as 1000 m of sediment (Syvitski and Praeg, 1989; Locat and Syvitski, 1991).

The Upper Saguenay Fjord is characterized by a Y-shape, with one arm of the Y being the Bras Nord and the other one being the Baie des Ha! Ha! (Fig. 3). The fjord, in that area, has water depths ranging from 0 to 275 m and a width between 3 and 5 km. The Saguenay River flows into the Bras Nord while the Mars, Ha! Ha! and du Moulin rivers flow into the Baie des Ha! Ha! The regular tide in the area is about 4–5 m. The most active segment of the upper Saguenay Fjord is the Bras Nord where the accumulation rate is measured in centimeters per year at the delta (Locat and Leroueil, 1988; Perret et al., 1995) so that the Bras Nord is being filled more rapidly that the Baie des Ha! Ha!, where sedimentation rates are of the order of 0.2 cm/yr (Barbeau et al., 1981a).

The water depth in the Bras Nord ranges from about 10 m at the mouth of the Saguenay River to 200 m at the confluence with the Baie des Ha! Ha! The Baie des Ha! Ha! itself has a water depth which rapidly increases to about 100 m near the head (at La Baie city) and to 200 m downstream. The floor of the Baie des Ha! Ha! has a unique feature located near the center, in the form of a sharp and more or less straight escarpment (arrows in Fig. 3). Above it, the slope is 0.6°, and below, 0.2°. The slopes on either side of the fjord are quite different, in particular in the Baie des Ha! Ha!, the northern sidewall is steep with slopes exceeding 40° while the south shore slope is gentler and gullied (Fig. 3). The slope on the

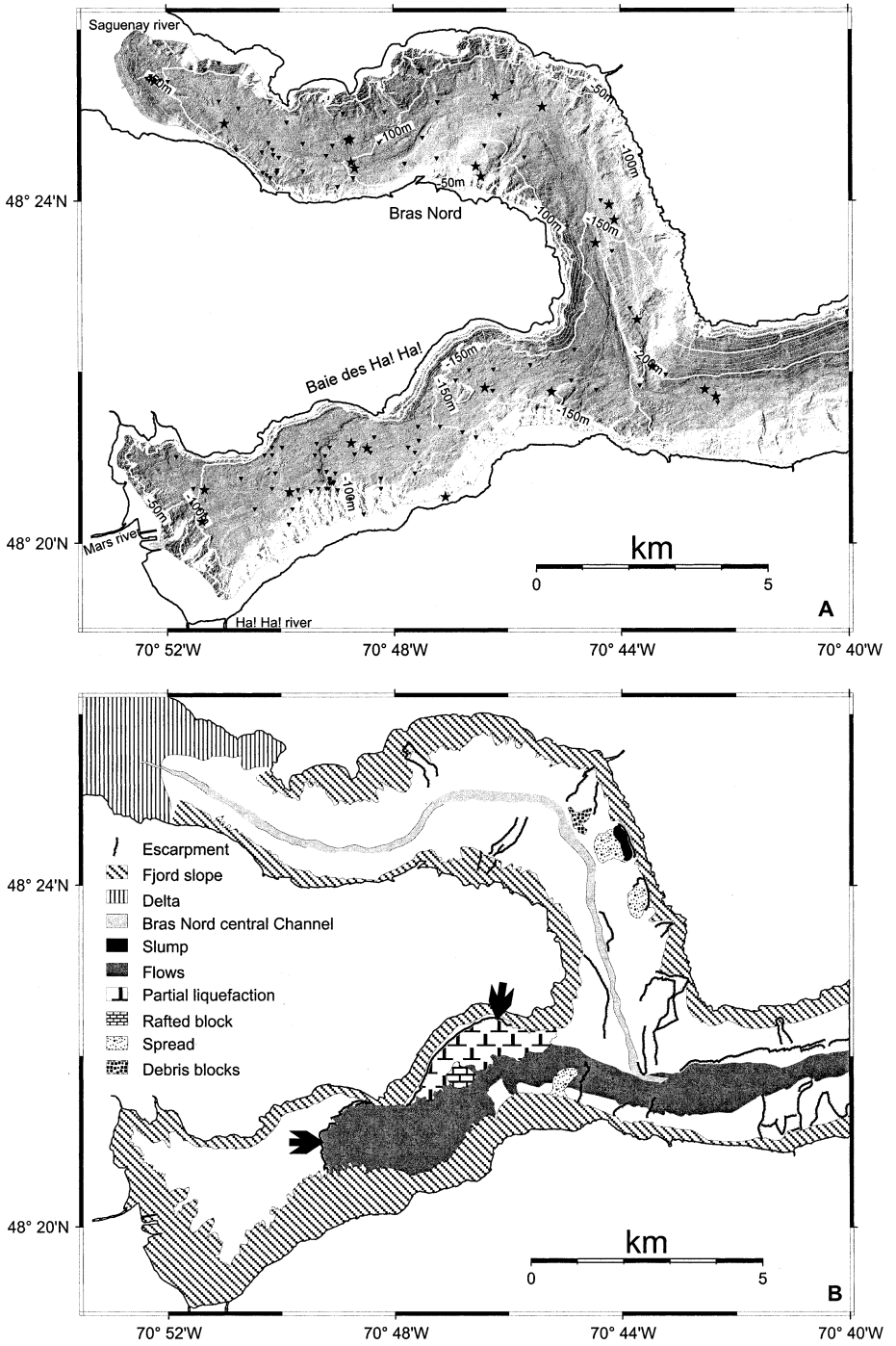


Fig. 3. (A) Bathymetry of the studied area with shaded relief illuminated from the West. Contours are also plotted at 5-m intervals between 0 and 100 m depth and 10-m intervals between 100 and 300 m depth. Box cores (inverted triangles) and Lehigh cores (stars) used in this study are also shown. (B) Geomorphological map of the Saguenay Fjord. Note abundance of escarpments and failure related deposits.

north side is controlled by the bedrock, while the southern side is dominated by Quaternary sediments. The Bras Nord is bisected by a shallow channel, which follows more or less the center of the fjord, potentially acting as a conduit for mud flows or debris flows originating from the upper reaches of the fjord (Fig. 3).

## 3. Methods

A seismic landslide hazard analysis results from the combination of a study of the seismic performance of a slope with a study of the seismic hazard. Both of these are considered in this paper through a Newmark (1965) analysis, and applied for spatial data using the Generic Mapping Tools (GMT, Wessel and Smith, 1991, 1998). Applying such a method using spatial data analysis is not new (see Jibson et al., 1998; Mankelow and Murphy, 1998; Miles and Keefer, 2000) and spatial data for the assessment of the sea floor stability have already been used (e.g. Mulder et al., 1994; Lee et al., 1999), but this is the first time the Newmark (1965) model has been applied to the submarine environment. The method has already been examined against a real landslide and it was found that measured displacements agreed quite well with calculated displacements (Wilson and Keefer, 1983). The model was implemented using the GMT grdmath module, which makes possible algebraic manipulation of grid files. All analyses were performed at a 20-m resolution. Usually, a flow control chart of a Newmark analysis would involve three major steps: (a) seismic shaking characterization, (b) assessment of the seismic landslide susceptibility, and finally, (c) integration of the two factors into an analysis of seismic landslide hazard that is expressed as permanent displacement (Miles and Keefer, 2000). These steps are described below in reverse order.

### *3.1. Seismic landslide hazard assessment: Newmark's method*

In this paper we use the Newmark (1965) analysis to calculate the displacement of a landslide under the action of seismic ground motion. In this method the slope is modeled as a friction block on an inclined plane subject to the same accelerations as the modeled slope. The displacement as considered in Wilson and Keefer (1983) is calculated from two inputs: the critical acceleration $a_c$ and a strong motion seismogram (Fig. 4A,E), a record of the seismic ground acceleration as a function of time $a(t)$. As long as $a(t)$ remains lower than $a_c$, the friction block remains stationary relative to the slope, if $a(t)$ surpasses $a_c$ then the block undergoes an acceleration, $a$, equal to:

$$a = a(t) - a_c \tag{1}$$

During this pulse the velocity of the block may be calculated by integrating the block acceleration over time (Fig. 4C,G). When $a(t)$ falls below $a_c$ again the block is still moving but is now decelerating until it stops (Fig. 4B,F). The block will not move again until $a(t)$ again surpasses $a_c$. Integrating the calculated velocities will yield the Newmark displacements (Fig. 4D,H).

It must be noted here that the term 'permanent displacement', as used in the sense of Wilson and Keefer (1983), differs from the occurrence of complete 'failure'. This recognizes that a finite amount of permanent displacement may precede full disruption of the ground surface. This agrees with the observational evidence that the transient effects of earthquake motions can induce some deformation on slopes prior to complete failure.

### *3.2. Seismic landslide susceptibility analysis and data collection: calculating the critical acceleration*

In the Newmark (1965) analysis the resisting force is represented by a critical or yield acceleration. Several similar approaches and simplifications exist to calculate the critical acceleration (e.g. Newmark, 1965; Sarma, 1975), but a common procedure is to let the critical acceleration equal the pseudostatic acceleration that produces a factor of safety of 1. In the pseudostatic approach it is assumed that the acceleration is applied over such a long period of time that the induced stresses can be considered constant (Hampton et al., 1996). In this study the critical

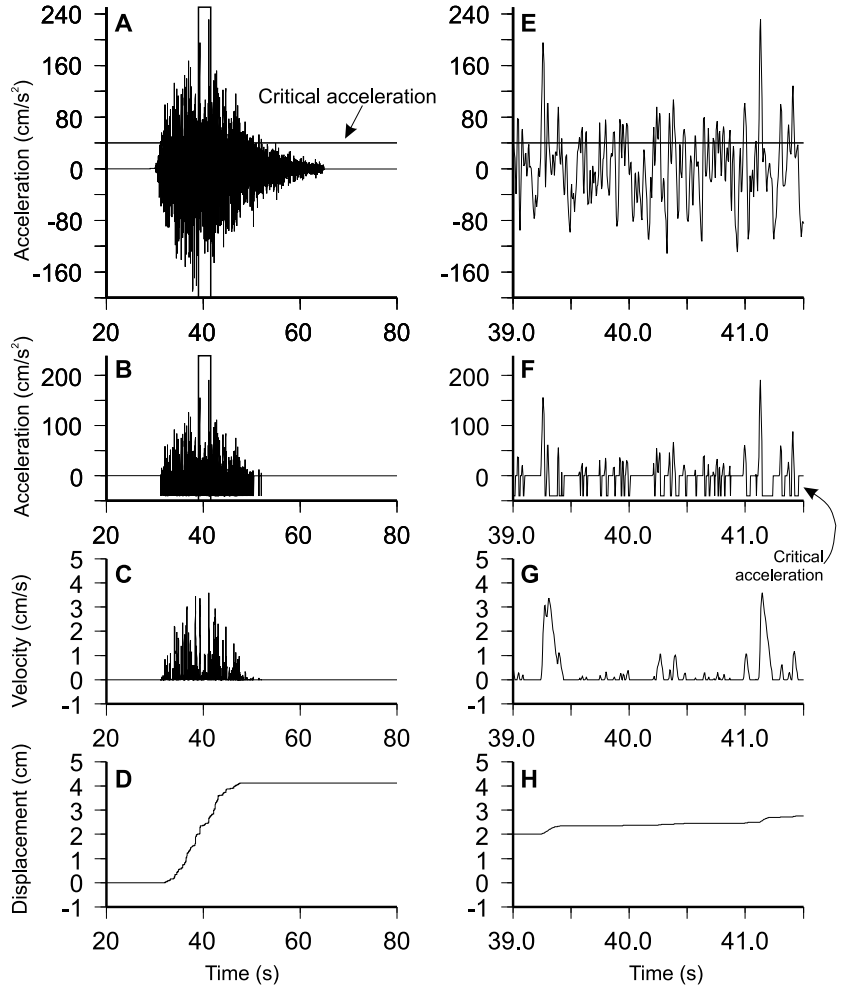


Fig. 4. (A) Example of synthetic seismogram for a 6.5-$M_w$ earthquake at an epicentral distance of 40 km with local site conditions as illustrated in Table 2. The example illustrates: (B) The accelerations applied to the block resulting from the interaction between moving forces (ground motion) and resisting forces simulated here as the critical acceleration. Note that in this example, we model a critical acceleration of 40 cm/s$^2$. (C) Calculated velocities. (D) Newmark displacement. (E–H) Zoom of the interval contained within a box in A.

acceleration is determined using the methodology of Lee and Edwards (1986) and Lee et al. (1999), which is appropriate for the marine environment and the difficulties associated with underwater sampling. The method considers three factors influencing slope stability (Lee et al., 1999): (1) lithology (as represented by mineralogy and grain size or engineering classification); (2) consolidation stress history due to erosion events (presence of sustained static shear stress, and existence of excess pore water or gas pressures); and (3) the nature of loading (static gravitational or cyclic). In the present study, the data available for calculating the critical acceleration on a spatial basis consists of EM1000 multibeam bathymetry and a database of sediment samples on which several physical properties were measured. The latter included 110 box cores and 28 gravity cores obtained using a 3-m-long Lehigh corer. In most box cores measurements were done at intervals of 1 cm and include corrected water content and undrained intact and remolded shear strength,

while on gravity cores, measurements were made at intervals ranging between 10 and 20 cm.

### 3.2.1. Lithology

The surficial sediments of the Saguenay Fjord appear to be quite homogeneous with an average grain size distribution of 26% clay, 71% silt and 3% sand. This distribution does not vary in a significant manner longitudinally (i.e. from proximal to distal areas), although a few of the more proximal samples show large sand contents and there is a slight decrease in silt content accompanied by a slight increase in clay content eastwards (Fig. 5).

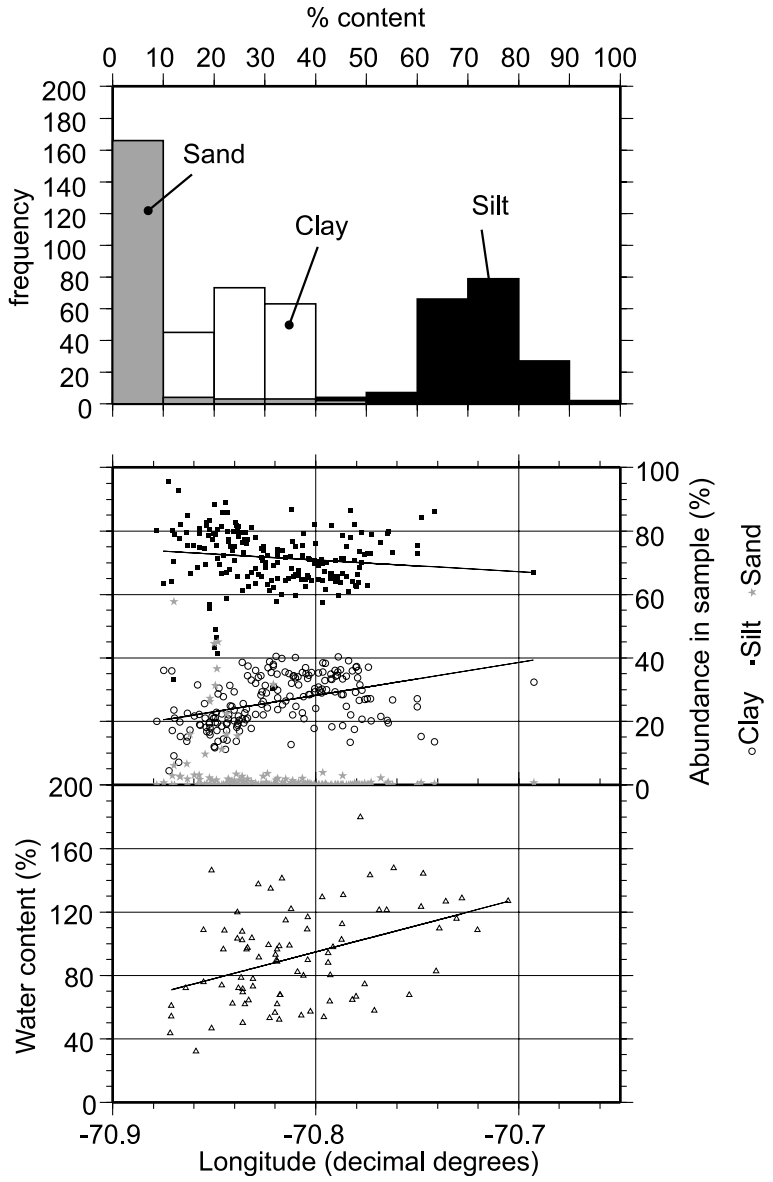


Fig. 5. Grain size distribution as measured in grab samples for the entire studied area (top), variability with longitude, i.e. from proximal to distal areas of the grain size (middle), and water content (bottom) (based on data from Urgeles et al., 2002).

The box cores show that the 1996 event layer has similar physicochemical characteristics to the rest of the Saguenay Fjord sediments (Maurice et al., 2000). The Lehigh cores show an overall trend with the water content decreasing with depth in sediment, while the shear strength increases (Fig. 6).

For the purpose of spatial analysis, Lee et al. (1999) and Lee and Baraza (1999) showed that sediment density from the near surface is a good indicator of engineering classification (see also Lee and Baraza, 1999). Therefore a map of near surface water content (Fig. 7), which is directly related to sediment density in fine marine sediments, is considered a good representation of the sediment's engineering classification. To this purpose the values of water content observed at 10 cm were gridded to produce such a map. The value of 10 cm was chosen following Lee et al. (1999) because it is considered to be below the zone of most active bioturbation but is still representative of the sediment lithology deposited most recently.

### 3.2.2. Consolidation stress history

The soil consolidation state is usually defined using the overconsolidation ratio (OCR), which is defined as the ratio of the vertical effective overburden stress ($\sigma'_v$), to the effective preconsolidation stress ($\sigma'_p$), the latter being a measure of the maximum stress applied to the sediment since deposition. Perret et al. (1995) showed that, in the Saguenay Fjord, when the sediment shear strength is normalized against the preconsolidation pressure, a value of 0.3 or 0.5 was obtained depending on whether the sediment contained less than 3% organic matter or more. The results of Perret et al. (1995) showed that, typically, the fjord sediments are overconsolidated in the upper half meter of the sediment column and are normally consolidated at greater depths. Such a superficial, apparent overconsolidation is very typical of marine sediments (Lee and Edwards, 1986; Cochonat et al., 1992), and its effects tend to disappear within the first meter of sediment column (Perret et al., 1995). Thus, in this study we consider that the Saguenay Fjord sediments are normally consolidated (OCR = 1), although near surface sediment samples show elevated levels of overconsolidation (OCR > 1).

Such surficial overconsolidation is clearly shown in Fig. 6B. The shear strength versus ver-

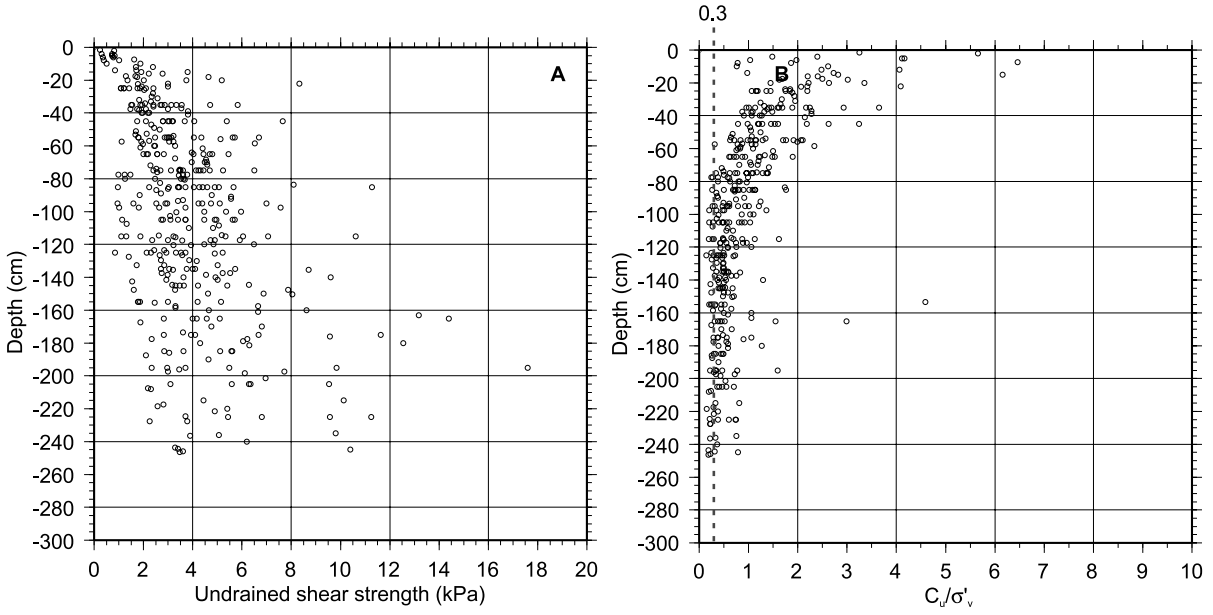


Fig. 6. (A) Undrained shear strength measured using the fall cone test versus depth. (B) The ratio of undrained shear strength/vertical effective stress versus depth for all Lehigh cores in the study area.

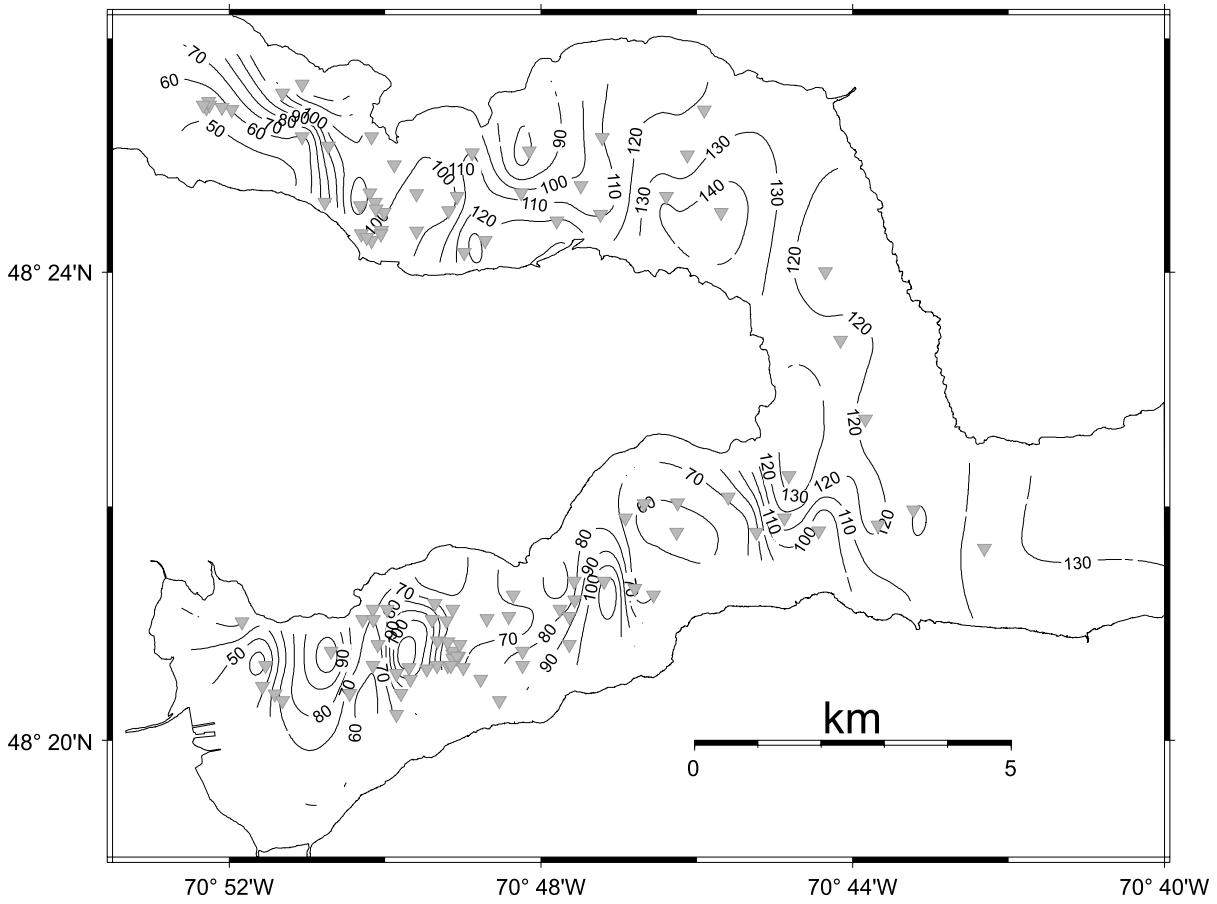


Fig. 7. Water content (%) at 10 cm depth using the adjustable tension continuous curvature surface gridding algorithm of Smith and Wessel (1990). Box cores (inverted triangles) used for gridding are also shown.

tical effective stress ratio in the Lehigh cores shows very high values in the first half meter of the sediment column, and then the values from all core samples become concurrently asymptotic to a value of $\sim 0.3$. Note that for normally consolidated sediments, the preconsolidation pressure equals the vertical effective stress.

### 3.2.3. Loading characteristics

The final two parameters needed to perform a seismic landslide susceptibility analysis are slope angle and the depth to failure for each potential landslide. Slope estimates were made from 20-m-resolution swath bathymetry grids (Fig. 8).

Considering all of the above factors, the shear stress induced by seismic and gravitational loading ($\tau_c$) on an infinite slope is (Lee and Edwards, 1986; Lee et al., 1999):

$$\frac{\tau_c}{\gamma' h} = \sin\alpha + \frac{a}{g}\frac{\gamma}{\gamma'} \tag{2}$$

where $\gamma$ and $\gamma'$ are respectively the total unit weight and the submerged unit weight of sediment, $\alpha$ is the slope angle, $h$ is depth in sediment, $g$ is the acceleration of gravity, and $a$ the horizontal pseudostatic earthquake acceleration. Vertical acceleration is neglected since, although earthquakes generate both horizontal and vertical accelerations that induce the corresponding shear and normal stresses in the sediment, it is mostly the shear stress that can drive the sediment to failure and responds most strongly to horizontal

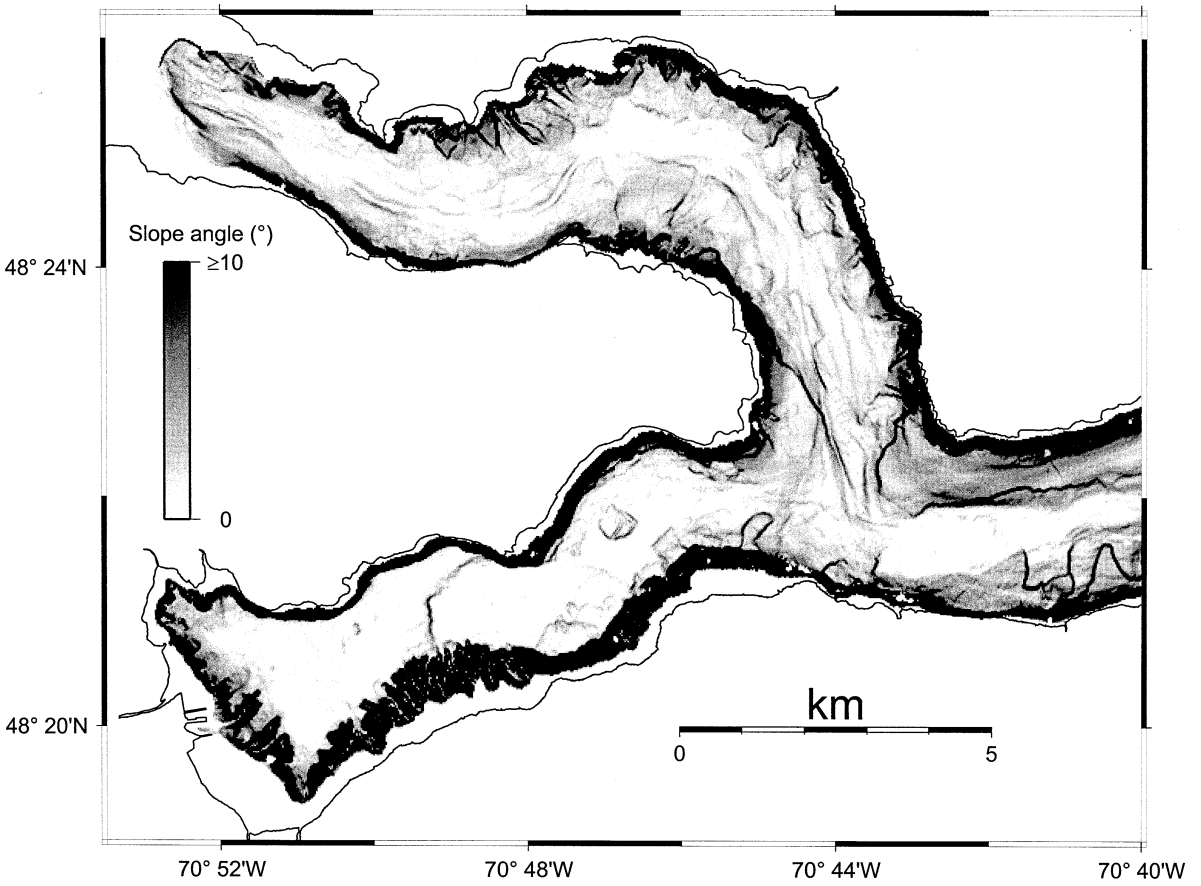


Fig. 8. Slope map of the Saguenay Fjord.

acceleration (Mulder et al., 1994; Hampton et al., 1996). It must be noted also that Eq. 2 is only used for slopes $< 10°$ (Lee and Edwards, 1986). This is not a major obstacle in this scenario, because the fjord slopes exceeding this value generally consist of rock outcrops.

Note that because of the surficial, apparent overconsolidation the relation $\gamma'/\gamma$ cannot be directly estimated from the water content measurements made on the uppermost box core sediments. Most of the cores show an overall increase of the $\gamma'/\gamma$ ratio with depth following an exponential trend. The cores with a higher $\gamma'/\gamma$ ratio on the seabed are those with higher $\gamma'/\gamma$ at depth (Fig. 9) and this relation is used to overcome the effect of the surficial, apparent overconsolidation. According to oedometer tests (Perret et al., 1995), normal consolidation occurs from 1 m onwards, although, from Fig. 6B we choose a depth of 1.2 m. Fig. 9 shows the relation between $\gamma'/\gamma$ at 10 cm and $\gamma'/\gamma$ at 1.2 m.

The correlation between surface measurements of $\gamma'/\gamma$ and those at depth is obviously complicated by the fact that we are considering a homogeneous non-layered system, while actually the system is a layered one. The cores north of 40.4°N, i.e. the most proximal areas of the Bras Nord, show the presence of a coarse turbidite layer related to the 1971 St. Jean de Vianney landslide (Schafer and Smith, 1988). This layer contrasts with that of the 1996 event, which looks much more similar to the background sedimentation. Such cores show an anomalous water content profile (see fig. 14 of Perret et al., 1995), and are therefore not used for the correlation. This profile seems to indicate that the 1971 material

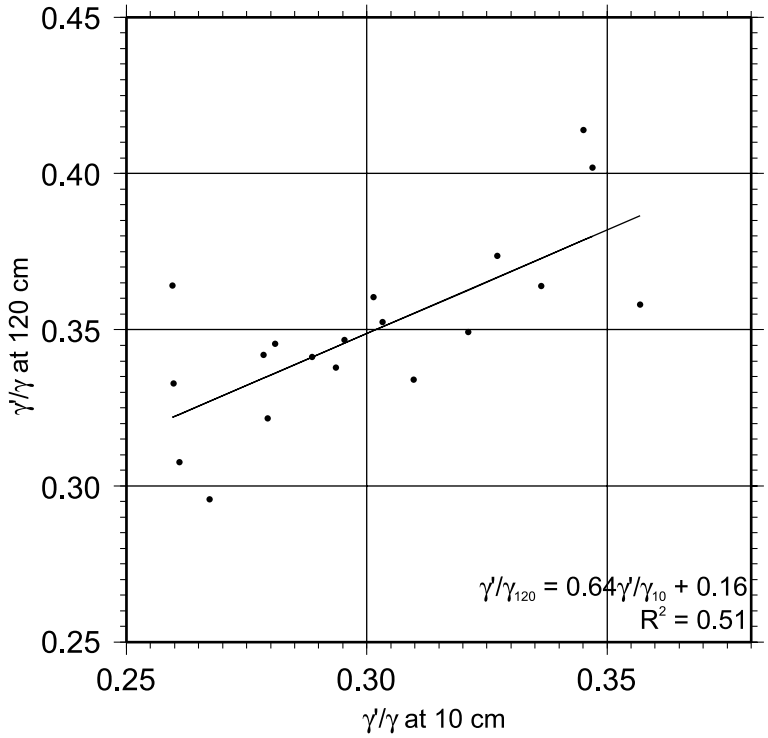


Fig. 9. The ratio of mean buoyant total unit weight at a depth of 120 cm to that at 10 cm as measured in Lehigh cores.

isolated the former surficial sediments which were already overconsolidated. This overconsolidation is again considered apparent and its influence lost with depth.

The advantage of using normalized parameters in Eq. 2 is that strength and stress normalization procedures provide results that are conceptually independent of subbottom depth. Results at depth are rigorously applicable if sediment lithology does not vary significantly and the consolidation state can be estimated (Lee and Edwards, 1986). Expressing the results in a normalized manner allows approximate extrapolation of test results below the limited depth of sampling allowed with a corer.

The cyclic shear stress ($\tau_c$) divided by the consolidation stress ($\sigma'_c$), termed the cyclic shear stress ratio (CSR) (Lee et al., 1999), shows a linear trend when plotted versus the $\log_{10}$ of the number of cycles to failure (Fig. 10). For fine marine sediments with different water contents it can be observed that for a specific number of significant cycles leading to failure (number of cycles with amplitude $\geq 0.65$ times the peak ground acceleration, the maximum horizontal acceleration measured at a site) the CSR required to cause failure increases with water content (Fig. 11). The method of Lee and Edwards (1986) has an additional advantage that allows overcoming one of the major problems of the Newmark (1965) analysis. As the method uses cyclic shear strengths to determine the critical acceleration, the strain softening behavior of most marine sediments can be accounted for. According to this, we should be able to calculate the CSR required to cause failure at each grid node as a function of the number of cycles observed or calculated (see 3.3. Calculating the seismic ground acceleration) at the corresponding distance from the epicenter. However, this largely complicates the calculation since it involves a decreasing value of $a_c$ with increasing number of cycles and time. Thus, for simplifica-

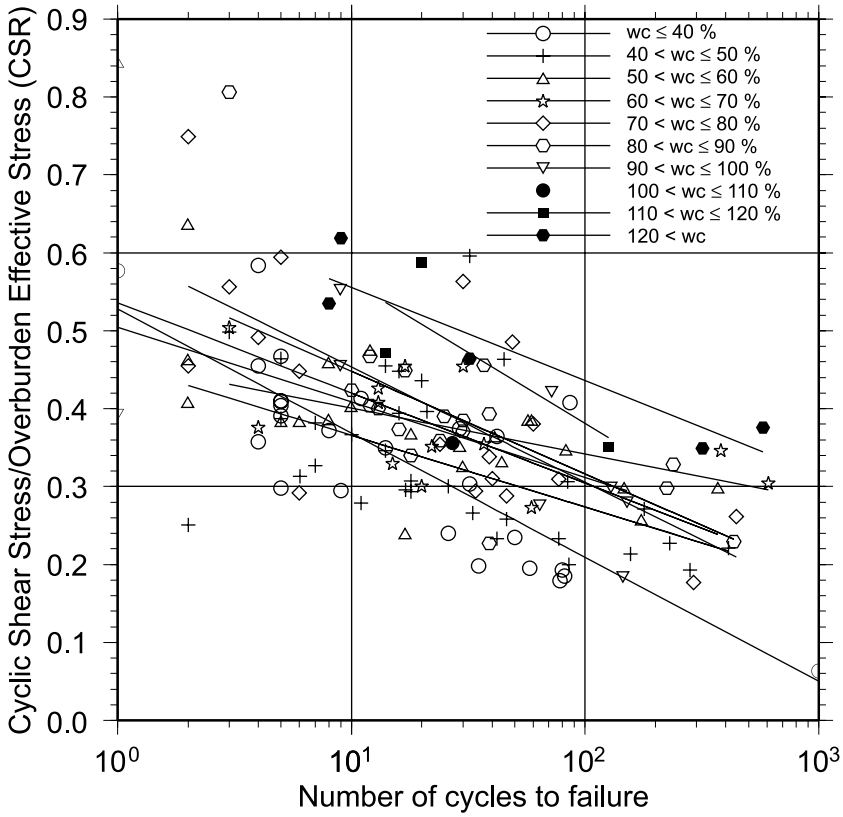


Fig. 10. Cyclic shear stress normalized by CSR versus number of cycles to failure (15% strain) from 144 cyclic triaxial tests performed on sediment from ten marine study areas distributed worldwide. Data points are identified according to initial water content ($w_c$) of the sediment tested (data from Lee et al., 1999).

tion purposes, we consider a unique value of the number of significant cycles although this may induce an overestimation of the displacement, which we think more suitable than the typical underestimation associated with the classical method (Kramer, 1996). Accordingly, we estimate that 16 is an appropriate value for the number of significant cycles leading to failure. This corresponds to the average number of cycles observed at distances between 60 and 90 km from the epicenters of the November 25, 1988, 5.8-moment magnitude ($M_w$) Saguenay earthquake (Lefebvre et al., 1992). It is worth remarking that the 1988 Saguenay earthquake is the most significant event over the last 50 years in eastern Canada, and it was the first earthquake of significant magnitude whose resulting ground motions were well recorded, providing valuable information to update seismic hazards (Tso and Zhu, 1991). For a factor of safety of 1.0, the normalized shear stress, $\tau_c/\sigma'_c$, is equal to the CSR at failure or $CSR_{16}$ (the CSR needed to cause failure in 16 cycles) for this application. Inserting $CSR_{16}$ in Eq. 2 and solving for the pseudostatic acceleration yields:

$$a_c = \frac{\gamma'}{\gamma}[CSR_{16} - \sin\alpha]g \quad (3)$$

where $a_c$ is the critical horizontal acceleration.

Plotting the mean of each water content grouping versus $CSR_{16}$ shows that the best fit (highest correlation factor) is linear (Fig. 11). These relations allow us to create input grids that are manipulated using Eq. 3 to generate a critical acceleration grid (Fig. 12).

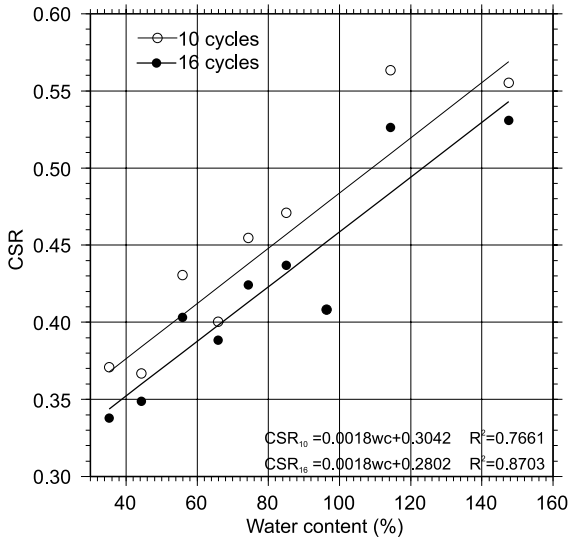


Fig. 11. The CSR producing failure in 10 and 16 cycles versus initial sediment water content. Data points are obtained from the intercept of these values of the number of cycles with the regressions for different water contents in Fig. 10.

### 3.3. Calculating the seismic ground acceleration

Selection of a time history for predictive hazard analysis can pose a major obstacle in using the double integration approach (Miles and Keefer, 2000). Ideally, records of an earthquake that occurred on the fault zone of interest having adequate magnitude to predict are used. Unfortunately, in many, if not most cases, such records do not exist. The alternatives consist of modifying actual records from the fault zone of interest (or another fault system) or generating artificial time histories. This issue is treated in more detail by Miles and Ho (1999) and Kramer (1996).

In addition, one must select a representative earthquake epicenter and magnitude. In our case we assumed that the source of major earthquakes in the Saguenay region is the epicenter of the well-known 1988 Saguenay earthquake (see Sommerville et al., 1990; Du Berger et al., 1991). This is consistent with the observation of a deep cluster of seismic events around the area of the 1988 Saguenay earthquake (Fig. 1B), and the lack of major faults along which earthquakes have occurred (see also Du Berger et al., 1991). Some authors also believe that the large amount of evidence for major slope instabilities in the Saguenay region associated with the local magnitude ($M_n$) $\sim$7 seismic event of 1663 (e.g. LaSalle and Chagnon, 1968; Syvitski and Schafer, 1996; Locat et al., 1997), the largest seismic event recorded in historical times in Quebec, is reason enough to believe that the actual epicenter of this event was not located in the Charlevoix region, but near the epicenter of the 1988 Saguenay earthquake (Locat et al., 2000). Thus, we decided to test the model against different earthquake magnitudes.

In this study, displacements were computed from synthetic time histories, which were iteratively created for each grid node. The seismic ground acceleration time histories were generated using a slightly modified version of the td_drvr SMSIM program (Boore, 1996), using the ground motion model of Atkinson and Boore (1995). The simulations were run using the parameters listed in Table 1. An aspect that we were careful to integrate in our computations was the local site condition, which has been demonstrated to have an important influence on ground motion characteristics (Wilson and Keefer, 1983; Idriss, 1990; Sugito et al., 1991).

The principal factors controlling local site conditions are topography (Wilson and Keefer, 1983; Benites and Aki, 1994) and the presence of soft soils (Idriss, 1990; Sugito et al., 1991). Unfortunately, we were not able to account for site effects due to the topography, which are probably quite important at the fjord margins. On the other hand we modeled local soil conditions using amplification factors computed by Herrmann and Akinci's (1999) dorvt180 program. The input soil stratig-

Table 1
Parameters used to conduct Boore (1996) simulation

| | |
|---|---|
| Stress drop | 100 bar |
| Cutoff frequency | 50 Hz |
| Free surface factor | 2 |
| Radiation pattern | 0.55 |
| Energy partition factor | 0.707 |

Based on Atkinson and Boore (1995) for eastern North American earthquakes.

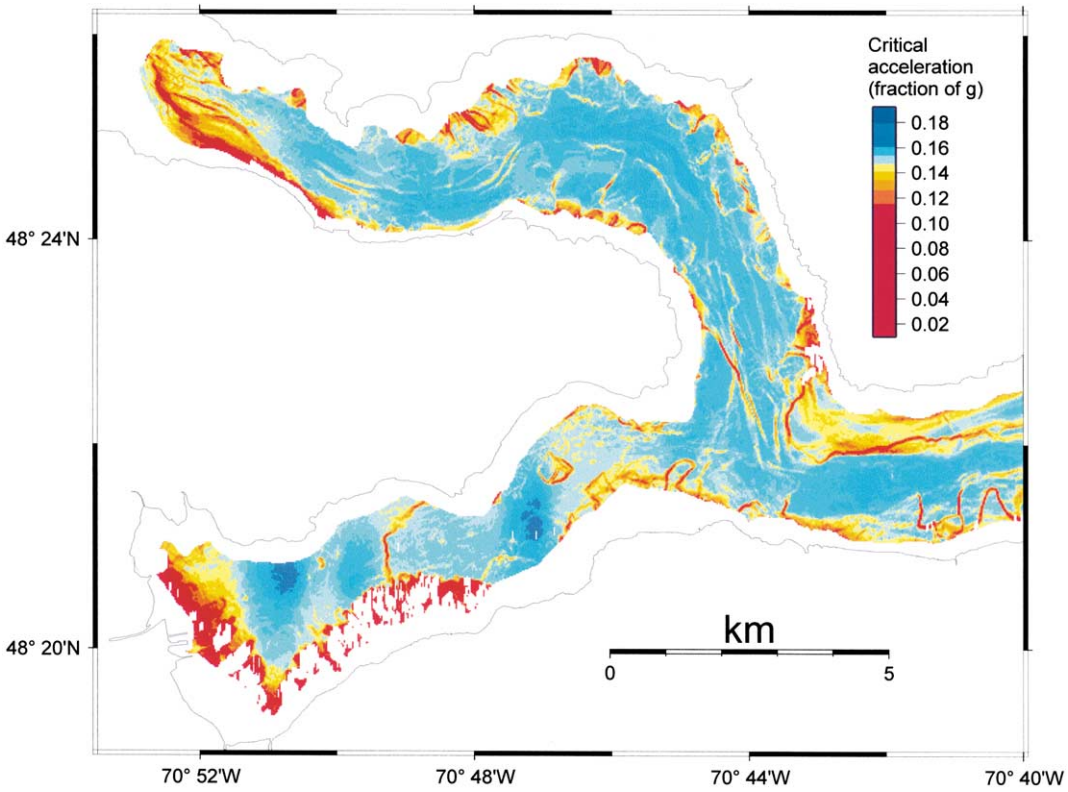


Fig. 12. Calculated critical horizontal earthquake acceleration (as a fraction of $g$) to cause shallow seated landslides in the Saguenay Fjord.

raphy, obtained from Locat and Syvitski (1991), consisted of a Precambrian basement overlain first by a 150-m-thick contact glacial till unit, second by a 100-m-thick proglacial till unit (see Table 2 for physical properties used in this study), and ultimately by an upper layer consisting of the Laflamme sea clays and Recent sediments. According to seismic reflection data (Locat and Syvitski, 1991), for this later unit we assume a variable thickness ($T$) controlled by the following function:

$$T = 1.85e^{3.28\cos\alpha} \quad (4)$$

where $\alpha$ is the slope angle. Such a function yields values between 50 m thickness (maximum estimated thickness of Laflamme sea clays and Recent sediments in the Saguenay Fjord) for flat surfaces (bottom fjord) and almost no sediment

Table 2
Input soil stratigraphy based on Locat and Syvitski (1991) and soil parameters based on Carr et al. (1998)

| Layer | $T$ (m) | $V_p$ (m/s) | $V_s$ (m/s) | $Q_s$ | $Q_p$ | $\rho$ (g/cm$^3$) |
|---|---|---|---|---|---|---|
| Recent and Laflamme sea clays | $1.85\ e^{3.28\cos\alpha}$ | 1800 | $250\ z^{0.18}$ | $6\ z^{0.24}$ | $6\ z^{0.24}$ | $0.8\ \log_{10}(v_s)-0.1$ |
| Proglacial till | 100 | 1500 | 420 | 500 | 500 | 2.0 |
| Contact till | 150 | 1600 | 450 | 500 | 500 | 2.1 |
| Precambrian basement | – | 6000 | 3500 | 500 | 500 | 2.7 |

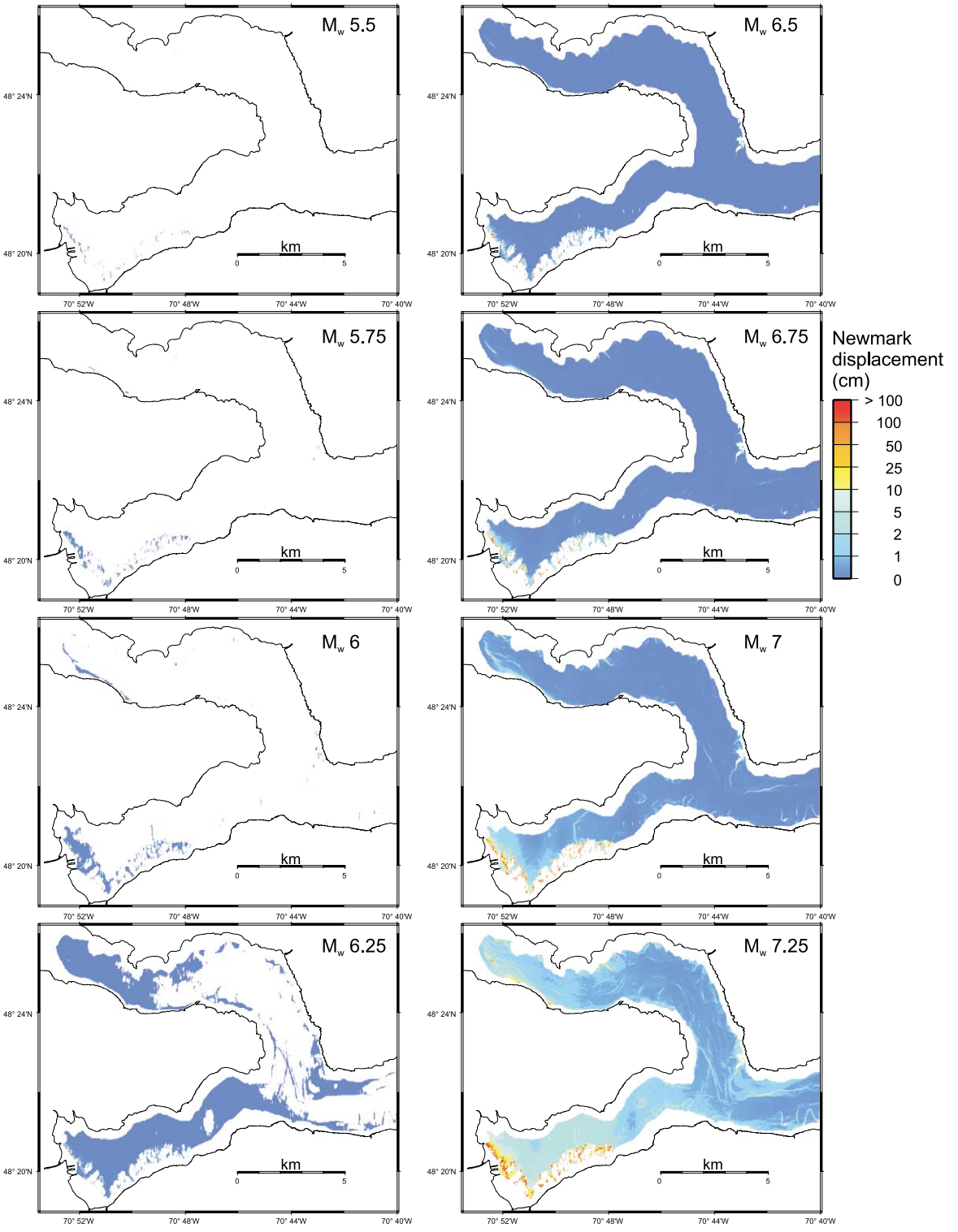
M$_w$ 5.5
M$_w$ 6.5
M$_w$ 5.75
M$_w$ 6.75
M$_w$ 6
M$_w$ 7
M$_w$ 6.25
M$_w$ 7.25
Newmark displacement (cm)
> 100
100
50
25
10
5
2
1
0
km
0
5
48° 24'N
48° 20'N
70° 52'W
70° 48'W
70° 44'W
70° 40'W

Fig. 13. A series of calculated Newmark displacements for increasing earthquake magnitudes. Simulations were run with an epicenter corresponding to that of the 1988 Saguenay earthquake.

cover for the fjord walls where gradients approach vertical.

## 4. Results

### 4.1. Slope gradients

The slope gradient strongly influences slope stability. The data derived from the multibeam echosounder show that the slopes within the fjord floor vary from almost 0° to more than 40°. The steepest slope gradients are associated with the fjord margins, but not all slopes can be treated in the same manner for the analysis of slope stability since, generally, the slopes exceeding 10° are rocky in nature.

There are also important changes in slope gradient within the deepest part of the fjord, where the bottom is covered mostly by sediment but slopes do not generally surpass 10°. The highest slope gradients within the deeper parts of the fjord are associated with linear features corresponding to escarpments related to landslide processes or channel erosion. There are also relatively strong gradients at the foot of the fjord walls where there is an input of sediment associated with the fjord margins.

### 4.2. Water content

The map of water content, $w_c$ (Fig. 7), will directly influence the estimated CSR needed to cause failure. The values range from about 50% to 150% of the dry weight. A general increase in water content is seen from the more proximal areas to distal areas in the Bras Nord, while in the Baie des Ha! Ha! such a trend is not so clear, although low values are also present in the most proximal area. This distribution is roughly consistent with grain size distribution, i.e. the lower water contents correspond to more sandy sediments, even though the predominant fraction all along the fjord is silt (Fig. 5). The areas with higher water content (Fig. 7) will be those showing the higher CSR required for failure and, accordingly, the areas where most sandy material exists will be those most prone to failure.

### 4.3. Critical acceleration

The estimated values of $a_c$ range between as much as 0.2 $g$ and as little as 0.08 $g$ (Fig. 12). As explained above, the critical acceleration cannot be directly compared with estimates of peak ground acceleration, and the later is usually larger than $a_c$ (Seed, 1979). Having taken this into account, it can be seen that the calculated $a_c$ values clearly fall within the range of accelerations that would be reached during an earthquake of the same characteristics as the well documented 1988 Saguenay earthquake (Fig. 1C). It would therefore 'trigger' some amount of permanent displacement. These accelerations also clearly fall within the range of accelerations that will be exceeded in 50 years with a 10% probability (Frankel et al., 1996) (Fig. 1D).

The distribution of calculated $a_c$ in Fig. 12 allows us to infer which geological processes influence slope stability in the Saguenay Fjord. The critical acceleration map (Fig. 12) shows three types of regions with low values of $a_c$. The first one is associated with the steep slope margins of the fjord.

The second type region is associated with the deltaic sediment accumulations at the head of the major rivers entering the Fjord, i.e. the Saguenay, Ha! Ha! and Mars rivers. This occurs as a result of the relatively high slope angle associated with progradation of the delta front in the case of the Saguenay River, but also because of the lower water contents the sediments hold in this area.

The third type zone is related to a major liquefaction event associated with a fault and escarpment that bisect the Baie des Ha! Ha! into two parts (see also Locat et al., 2000). The map in

Fig. 12 shows moderate low values of $a_c$ just below the main scarp as well as further down, where the fjord floor shows a blocky morphology (arrows in Fig. 3B), probably resulting from a partial liquefaction of a section of a landslide.

### 4.4. Newmark displacements

Fig. 13 depicts Newmark displacements for different intensities of ground shaking. According to these data, earthquakes of $M_w \leq 5.75$ do not cause any significant displacement of the fjord sediments. On the other hand, displacements appear widespread for accelerations induced by earthquakes of $M_w > 6.5$. Major displacements occur mostly at the head of the Baie des Ha! Ha! and St. Fulgence delta, when the slopes are subjected to accelerations induced by earthquakes in excess of $M_w$ 6.75. Fig. 13 shows no major displacements for earthquakes with $M_w = 5.9$, which is consistent with the lack of major landslides in the fjord bottom associated with the Saguenay seismic event of 1988.

As explained above, a finite amount of permanent displacement may precede major disruption of the ground surface. Many works (see for example Wilson and Keefer, 1983) describe a critical displacement beyond which major failure will occur. Miles et al. (2000) note that such a critical displacement has not been rigorously studied and there is little consensus regarding what is a representative value. Mankelow and Murphy (1998) review several cases to show that values of critical displacement depend on the materials involved and the type of landslides. Critical displacements have ranged from 2 cm for rock falls through 5 cm for translational slides, block slides and slumps to 10 cm for deep-seated rotational slides (see Mankelow and Murphy, 1998). It is clear from the maps shown in Fig. 13 that the latter value is unable to explain the landslides in the Saguenay Fjord. Considering the type of failures observed in the Saguenay Fjord (Fig. 4), mostly shallow translational and rotational slides, we would expect values not exceeding 5 cm, however the displacements observed at 'reasonable' earthquake magnitudes (known to have occurred in the area) would indicate a slightly lower value, which probably represents the particularities of the submarine environment. There are several large landslides in the Saguenay Fjord, but their limited number does not allow us to recommend a value of critical displacement.

## 5. Discussion

### 5.1. Stability of the 1996 flood event layer

As mentioned above major displacements are only expected in certain regions of the fjord for moment magnitudes larger than 6.75. The areas that appear most likely to fail under such earthquakes are the head regions of the Baie des Ha! Ha! and the delta of St. Fulgence in the Bras Nord. As noted previously, some authors (e.g. Locat et al., 2000) believe that the $M_n \sim 7$ earthquake of 1663 might have had its epicenter somewhere near the epicenter of the 1988 Saguenay earthquake. If such an earthquake was to take place now, it would pose a major hazard to the stability of the flood layer. However, earthquakes of such magnitudes do not appear to be frequent in the Saguenay Fjord region. Lake sediment cores representing some 3000 years of sediment accumulation of the area near the Saguenay Fjord have shown the occurrence of 'abnormal' silt layers attributed to seismic shaking events prior to the 1988 earthquake (Doig, 1998). The silt layers, much thicker and more widely distributed than the one associated with the 1988 event, were believed to be generated by earthquakes of local origin of magnitudes ranging between 6 and 7. From these data Doig (1998) estimated a recurrence interval for magnitude $\geq 6$ earthquakes of 350–1000 years. Thus, it would appear from this recurrence interval range that failure of the flood layer in the near future is highly unlikely.

### 5.2. Contrasting the model results with geological and geomorphological evidence

The critical acceleration and Newmark displacement charts show results that are consistent with geological and geomorphological observations. First of all, the areas that seem most prone

to failure are those more proximal to river mouths where slopes are steep, cohesionless materials are present, and sedimentation rates are high. The agreement is striking between relatively low values of the critical acceleration and the location the largest failure in the fjord (Fig. 3A,B, arrows), roughly in the center of the Baie des Ha! Ha! (Fig. 12). This might indicate that failure took place in an area where sediments already had low cyclic shear strengths.

### 5.3. Influence of local site conditions

One of the major influences on ground motion is local site condition. This is a factor that, if not properly taken into account, may strongly affect estimates of Newmark displacement. For example, ground motions generated by moderate earthquakes at distances of 40–100 km may be amplified by a factor of two by site characteristics (Idriss, 1990). When we initially carried out our study, we evaluated ground motions as they would occur on firm rock, and deceivingly the results could not explain how landslides could be formed on the fjord bottom without seismic events of an extraordinary magnitude. However, if amplification is considered, inferred ground motions and displacements may be explained from the range of earthquakes that the area is known to be subject to from historical records.

### 5.4. Method limitations

Several simplifications are implicit in the analysis we have carried out. Among them, the simplification that may most influence results relates to the input parameters used to calculate the critical acceleration ($a_c$). In our analysis we assumed that Recent Saguenay sediments behave the same as most present marine sediments. While this is a reasonable approximation it is also true that sedimentation in fjord areas has a specific character that probably affects their geotechnical properties. Some authors (see Yegian et al., 1991a,b; Mankelow and Murphy, 1998) include a probabilistic approach to account for the variability and uncertainty associated with the input parameters. Although such an analysis is desirable, it is beyond the scope of this paper. There is an additional uncertainty derived from the model of Lee and Edwards (1986). The model assumes that the sediment is vertically homogeneous while, actually, we should probably best consider a layered system as shown by down core variations of the grain size, water content and shear strength.

A complete discussion of the limitations of spatial analysis for determining earthquake induced landslide hazard is given in Miles et al. (2000). The major limitation we are dealing with in spatial data analysis when combining data sets such as bathymetry derived from multibeam sonar systems and physical properties measured on samples is the fact that the data sets have resolutions that differ by orders of magnitude. Transforming the data measured on sediment samples to a higher resolution data set involves deaggregation, which will cause an added uncertainty (Heuvelink and Pebesma, 1999). Miles et al. (2000) note that that this consideration implies that we should run the analysis at the resolution of the coarsest data. However, we proceeded, as did Miles et al. (2000), with the most common choice of using the resolution of the bathymetry data.

A problem of the Newmark's analysis is that the effects of the vertical component of shaking are not accounted for (Jibson, 1993).

Although, as noted by Miles and Keefer (2000), synthetic ground motion may not accurately predict actual ground motions in all instances, this method is considered the most reliable since it does not rely on extrapolations based on data from other areas.

### 5.5. Future work

To assess the stability of the 1996 flood layer with more confidence, further samples need to be acquired to overcome, at least to a larger extent, the problems associated with deaggregation.

We assume that the cyclic response of the sediments in Fig. 10, which are derived from study areas worldwide, is approximately the same as the response of Saguenay Fjord sediments. Tests under cyclic load conditions also need to be carried out on Saguenay Fjord sediments to determine the consistency of such an assumption.

## 6. Conclusions

In this article we apply spatial data and extend the pseudostatic approach of Lee and Edwards (1986), to perform a Newmark permanent displacement analysis using synthetic ground motions. The analysis produces a consistent agreement between calculated Newmark displacements, critical acceleration and present or most likely areas of slope instability.

Amplification due to specific soil conditions appears to be an important parameter to take into account if reliable earthquake magnitudes are to be linked with landslides in the study area. Such amplification will efficiently control the ground motion characteristics and, thus, the onset of landslide triggering.

According to this study, major displacements that might induce failure are only expected from earthquake moment magnitudes of 6.5 or larger. Therefore, the 1996 flood layer appears to be seismically stable.

## Acknowledgements

The authors would like to thank the several captains and crews of the vessels involved in acquiring the data here presented, including those of F.G. Creed, D. Riverain and A.C. Horth. We also owe thanks to P. Cochonat, M. Makelow and T. Mulder for critically reviewing the manuscript. We acknowledge the financial support of the Quebec Ministry of Education for postdoctoral fellowship provided to R.U. This study was supported by the Natural Sciences and Engineering Research Council and Alcan of Canada Ltd with funds provided to the strategic project 'Saguenay post-déluge' (STP201981) and COSTA-Canada (CRO-234277-00). Support from the EU through project COSTA (EVK3-CT-1999-00006) is also acknowledged.

## References

Atkinson, G.M., Boore, D.M., 1995. Ground-motion relations for eastern North America. Bull. Seismol. Soc. Am. 85, 17–30.

Barbeau, C., Bougie, R., Côté, J.-E., 1981a. Varations spatiales et temporelles du césium-137 et du carbone dans des sédiments du fjord du Saguenay. Can. J. Earth Sci. 18, 1004–1011.

Barbeau, C., Bougie, R., Côté, J.-E., 1981b. Temporal and spatial variations of mercury, lead, zinc, and copper in sediments of the Saguenay fjord. Can. J. Earth Sci. 18, 1065–1074.

Benites, R., Aki, K., 1994. Ground motion at mountains and sedimentary basins with vertical seismic velocity gradient. Geophys. J. Int. 116, 95–118.

Boore, D.B., 1996. SMSIM – Fortran program for simulating ground motions from earthquakes: Version 1.0. USGS Open File Report 96-80-A. US Geological Survey, Denver, CO, 73 pp.

Bouchard, R., Dion, D.J., Tavenas, F., 1983. Origine de la préconsolidation des argiles du Saguenay, Québec. Can. Geotech. J. 20, 315–328.

Brooks, G.R., Lawrence, D.E., 1999. The drainage of the Lake Ha! Ha! reservoir and downstream impacts along Ha! Ha! River, Saguenay area, Quebec, Canada. Geomorphology 28, 141–168.

Carr, B.J., Hajnal, Z., Prugger, A., 1998. Shear-wave studies in glacial till. Geophysics 63, 1273–1284.

Chagnon, J.Y., Locat, J., 1988. The effects of seismic activity on the soils of the Charlevoix area – Quebec, Canada. In: El-Sabh, M.I., Murty, T.S. (Eds.), Natural and Man-made Hazards. Reidel, Dordrecht, pp. 125–136.

Cochonat, P., Le Suavé, R., Charles, C., Greger, B., Hoffert, M., Lenoble, J.P., Meunier, J., Pautot, G., 1992. First in situ studies of nodule distribution and geotechnical measurements of associated deep-sea clay (Northeastern Pacific Ocean). Mar. Geol. 103, 373–380.

Department of Earth and Planetary Sciences, 2000. Harvard Centroid Moment Tensor Database, Harvard University, Cambridge, MA, http://www.seismology.harvard.edu/CMTsearch.html.

Doig, R., 1998. 3000-year paleoseismological record from the region of the 1988 Saguenay, Quebec, earthquake. Bull. Seismol. Soc. Am. 88, 1198–1203.

Du Berger, R., Roy, D.W., Lamontagne, M., Woussen, G., North, R.G., Wetmiller, R.J., 1991. The Saguenay (Quebec) earthquake of November 25, 1988: seismologic data and geologic setting. Tectonophysics 186, 59–74.

Duperret, A., Bourgois, J., Lagabrielle, Y., Suess, E., 1995. Slope instabilities at an active continental margin: large-scale polyphase submarine slides along the northern Peruvian margin, between 5°S and 6°S. Mar. Geol. 122, 303–328.

Earth Resources Information Systems Data Center, 1996. Global 30 arc second elevation data set: Sioux Falls, SD. US Geological Survey, Denver, CO, http://edcwww.cr.usgs.gov/landdaac/gtopo30/gtopo30.html.

Frankel, A., Mueller, C., Barnhand, T., Perkins, D., Leyendecker, E.V., Dickman, N., Hanson, S., Hopper, M., 1996. National seismic-hazard maps: documentation June 1996. US Geological Survey Open-File Report, 96-532. US Geological Survey, Denver, CO, 71 pp.

Hampton, M.A., Lee, H.J., Locat, J., 1996. Submarine landslides. Rev. Geophys. 34, 33–59.

Herrmann, R.B., Akinci, A., 1999. Mid-America ground motion models, http://www.eas.slu.edu/People/RBHerrmann/MAEC/maecgnd.html.

Heuvelink, G.B.M., Pebesma, E.J., 1999. Spatial aggregation and soil process modelling. Geoderma 89, 47–65.

Idriss, I.M., 1990. Influence of local site conditions on earthquake ground motions. Proceedings of the Fourth US National Conference on Earthquake Engineering, Palm Springs, CA, 1, pp. 55–57.

Jibson, R.W., 1993. Predicting earthquake-induced landslide displacements using Newmark's sliding block analysis. Transp. Res. Rec. 1411, 9–17.

Jibson, R.W., Harp, E.P., Michael, J.A., 1998. A method for producing digital probabilistic seismic landslide hazard maps: An example of the Los Angeles, California, area. US Geological Survey Open-File Report 98-113. US Geological Survey, Denver, CO, 17 pp.

Kramer, S.L., 1996. Geotechnical Earthquake Engineering. Prentice-Hall, Englewood Cliffs, NJ, 653 pp.

LaSalle, P., Chagnon, J.-Y., 1968. An ancient landslide along the Saguenay River, Quebec. Can. J. Earth Sci. 5, 548–549.

LaSalle, P., Tremblay, G., 1978. Dépôts meubles Saguenay Lac Saint-Jean. Rapport Géologique 191. Ministère des Richesses naturelles du Québec, Québec, 61 pp.

Lee, H.J., Baraza, J., 1999. Geotechnical characteristics and slope stability in the Gulf of Cadiz. Mar. Geol. 155, 173–190.

Lee, H.J., Edwards, B.D., 1986. Regional method to assess offshore slope stability. J. Geotech. Eng. 112, 489–509.

Lee, H.J., Locat, J., Dartnell, P., Israel, K., Wong, F., 1999. Regional variability of slope stability: application to the Eel margin, California. Mar. Geol. 154, 305–321.

Lefebvre, G., Leboeuf, D., Hornych, P., Tanguay, L., 1992. Slope failures associated with the 1988 Saguenay earthquake, Quebec, Canada. Can. Geotech. J. 29, 117–130.

Locat, J., Bergeron, M., 1988. Étude à rebours de glissements sous-marins, fjord du Saguenay, Québec. Proceedings of the 41st Canadian Geotechnical Conference, Waterloo, ON, pp. 338–346.

Locat, L., Leroueil, S., 1988. Physicochemical and geotechnical characteristics of recent Saguenay Fjord sediments. Can. Geotech. J. 25, 382–388.

Locat, J., Syvitski, J.P., 1991. Le fjord du Saguenay et le golfe du St-Laurent: Étalons pour l'évaluation des changements globaux au Québec. In: Bouchard, M.A., Bérard, J., Delisle, C.E. (Eds.), Collection Environnement et Géologie, Vol. 12. Association Professionelle des Géologues et des Géophysiciens du Québec, Québec, QC, pp. 309–318.

Locat, J., Dubé, S., Couture, R., 1997. Analyse de l'écroupement rocheux du Mont Éboulé, Québec. Proceedings of the 50th Canadian Geotechnical Conference, Ottawa, ON, pp. 118–126.

Locat, J., Urgeles, R., Schmitt, T., Hoareau, L., Martin, F., Hill, P., Long, B., Simpkin, P., Kammerer, E., Sanfaçon, R., 2000. The morphological signature of natural disasters in the Upper Saguenay Fjord area, Québec, Canada. Proceedings of the 53rd Canadian Geotechnical Conference, Montreal, QC, pp. 109–116.

Loring, D.H., Bewers, J.M., 1978. Geochemical mass balance of mercury in Canadian fjord. J. Chem. Geol. 22, 309–330.

Mankelow, J.M., Murphy, W., 1998. Using GIS in the probabilistic assessment of earthquake triggered landslide hazards. J. Earthq. Eng. 2, 593–623.

Martel, L., Gagnon, M., Massé, R., Leclerc, A., 1987. The spatio-temporal variations and fluxes of polycyclic aromatic hydrocarbons in the sediments of the Saguenay fjord. Water Res. 21, 699–707.

Maurice, F., Locat, J. and Leroueil, S., 2000. Caractéristiques géotechniques et évolution de la couche de sédiments déposée lors du déluge de 1996 dans la Baie des Ha! Ha! (Fjord du Saguenay, Québec). Proceedings of the 53rd Canadian Geotechnical Conference, Montreal, Québec, pp. 125–132.

Miles, S.B., Ho, C.L., 1999. Rigorous landslide hazard zonation using Newmark's method and stochastic ground motion simulation. Soil Dyn. Earthq. Eng. 18, 305–323.

Miles, S.B., Keefer, D.K., 2000. Evaluation of seismic slope-performance models using a regional case study. Environ. Eng. Geosci. 6, 25–39.

Miles, S.B., Keefer, D.K., Nyerges, T.L., 2000. A case study in GIS-based environmental model validation using earthquake-induced landslide hazard, Proceedings of the 4th International Symposium on Spatial Accuracy Assessment in Natural Resources and Environmental Science, Amsterdam, pp. 481–492.

Mulder, T., Tisot, J.-P., Cochonat, P., Bourillet, J.-F., 1994. Regional assessment of mass failure events in the Baie des Anges, Mediterranean Sea. Mar. Geol. 122, 29–45.

Natural Resources Canada, 1999. Canadian national earthquake database, Ottawa, Canada. Geological Survey of Canada. http://www.seismo.nrcan.gc.cadatabase/eq_db_e.html.

Newmark, N.M., 1965. Effects of earthquakes on dams and embankments. Géotechnique 15, 139–160.

Perret, D., Locat, J., Leroueil, S., 1995. Strength development with burial in fine-grained sediments from the Saguenay Fjord, Quebec. Can. Geotech. J. 32, 247–262.

Piper, D.J.W., Cochonat, P., Morrison, M.L., 1999. The sequence of events around the epicentre of the 1929 Grand Banks earthquake: initiation of debris flows and turbidity currents inferred from sidescan sonar. Sedimentology 46, 79–97.

Roberts, J.A., Cramp, A., 1996. Sediment stability on the western flanks of the Canary Islands. Mar. Geol. 134, 13–30.

Sarma, S.K., 1975. Seismic stability of earth dams and embankments. Géotechnique 25, 743–761.

Schafer, C.T., Smith, J.N., 1987. Hypothesis for a submarine landslide and cohesionless sediment flows resulting from a 17th century earthquake-triggered landslide in Quebec, Canada. Geo-Mar. Lett. 7, 31–37.

Schafer, C.T., Smith, J.N., 1988. Evidence of the occurrence and magnitude of terrestrial landslides in recent Saguenay Fjord sediments. In: El-Sabh, M.I., Murty, T.S. (Eds.), Nat-

ural and Man-made Hazards. Kluwer Academic, New York, pp. 137–145.

Schafer, C.T., Smith, J.M., Loring, D.H., 1980. Recent sedimentation events at the head of the Saguenay Fjord, Canada. Environ. Geol. 3, 139–150.

Seed, H.B., 1979. Considerations in earthquake-resistant design of earth and rock-fill dams. Géotechnique 29, 215–263.

Smith, W.H.F., Wessel, P., 1990. Gridding with continuous curvature splines in tension. Geophysics 55, 293–305.

Sommerville, P.G., McLaren, J.P., Saikia, C.K., Helemberger, D.V., 1990. The 25 November 1988 Saguenay earthquake and the attenuation of strong ground motion. Bull. Seismol. Soc. Am. 80, 1118–1143.

Sugito, M., Kiremidjian, A.S., Shah, H.C., 1991. Nonlinear ground motion amplification factors based on local soil parameters. Proceedings of the International Conference on Seismic Zonation 2, Stanford, CA, pp. 221–228.

Syvitski, J.P.M., Praeg, D.B., 1989. Quaternary sedimentation in the St. Lawrence estuary and adjoining areas, Eastern Canada: an overview based on high-resolution seismo-stratigraphy. Géogr. Phys. Quat. 43, 291–310.

Syvitski, J.P.M., Schafer, C.T., 1996. Evidence for an earthquake-triggered basin collapse in Saguenay Fjord, Canada. Sediment. Geol. 104, 127–153.

Tso, W.K., Zhu, T.J., 1991. Implications of the 1988 Saguenay earthquake on Canadian seismic strength specification. Can. J. Civ. Eng. 18, 130–139.

Tuttle, M., Law, K.T., Seeber, L., Jacob, K., 1990. Liquefaction and ground failure induced by the 1988 Saguenay, Quebec earthquake. Can. Geotech. J. 27, 580–589.

Urgeles, R., Locat, J., Schmitt, T., Hughes Clarke, J.E., 2002. The July 1996 flood deposit in the Saguenay Fjord, Quebec, Canada: Implications for sources of spatial and temporal backscatter variations. Mar. Geol. 184, 41–60.

Wessel, P., Smith, W.H.F., 1991. Free software helps map and display data. EOS Trans. Am. Geophys. Union 72, 441.

Wessel, P., Smith, W.H.F., 1998. New, improved version of the Generic Mapping Tools released. EOS Trans. Am. Geophys. Union 79, 579.

Wilson, R.C., Keefer, D.K., 1983. Dynamic analysis of a slope failure from the 6 August 1979 Coyote Lake, California, earthquake. Bull. Seismol. Soc. Am. 73, 863–877.

Yegian, M.K., Marciano, E.A., Ghahraman, V.G., 1991a. Seismic risk analysis for earth dams. J. Geotech. Eng. 117, 18–34.

Yegian, M.K., Marciano, E.A., Ghahraman, V.G., 1991b. Earthquake-induced permanent deformations: Probabilistic approach. J. Geotech. Eng. 117, 35–50.